Article

Photovoltaic Electrification and Water Pumping Using the Concepts of Water Shortage Probability and Loss of Power Supply Probability: A Case Study

Misagh Irandoostshahrestani * and **Daniel R. Rousse**

Industrial Research Group in Technologies of Energy and Energy Efficiency (t3e), École de Technologie Supérieure (ÉTS), University of Quebec, Montreal, QC H3C 1K3, Canada
* Correspondence: misagh.irandoostshahrestani.1@ens.etsmtl.ca

Abstract: In this paper, a techno-economic investigation of a small-scale solar water pumping system combined with power generation is conducted numerically. Irrigation and power production for a typical small-size citrus farm located in southern Iran is simulated. The system consists of monocrystalline photovoltaic panels (CS3K-305MS, 305 W), absorbent glass material batteries (8A31DT-DEKA, 104 Wh), inverters (SMA Sunny Boy 2.0, 2000 W), and a pumping storage system. The key concepts of water shortage probability (WSP) and loss of power supply probability (LPSP) are used in conjunction with users' tolerances and sizing of the system. A genuine MATLAB code was developed and validated before the simulations. A specific electricity consumption pattern for a rural home and a variable irrigation water profile were considered. The main objective of the study is to size a system that provides both electricity for domestic use of a home as well as the energy required for running the irrigation pumps with respect to investment cost, LCOE, WSP, and LPSP. The main findings of the research are that LPSP and WSP threshold tolerances can have a preponderant effect on the cost and sizing of the system. Interestingly, results reveal that there is a minimum variation of the capital expenditure (CAPEX) versus the number of PV panels. For the optimal configuration, the study indicates that shifting from an LPSP of 0% to 3% (or about ten days of potential yearly shortage) makes the LCOE drop by about 55%, while the WSP decreases by about 36%.

Keywords: PV-powered system; electrification; water pumping; water shortage probability; loss of power supply probability; battery storage; Irrigation

1. Introduction

Worldwide, the need for energy is expanding globally as the population and average energy consumption per capita are both increasing [1]. Nowadays, both the private and public sectors are trying to use renewable and sustainable energy sources to meet their needs. Among other renewable sources, the solar photovoltaic system has been used since 1954 when Chapin, Fuller, and Pearson developed the silicon photovoltaic (PV) cell [2]. Lots of studies have been done since then to increase the efficiency of PV panels. Nevertheless, the turning point in using this energy source is the drastic drop in the technology cost along with the increase in reliability and durability of systems [3,4]. Since 2020, several calls for tenders for power production have been won by bids involving solar PV, thus dethroning fossil fuel power plants. More than ever, this makes PV panels an attractive alternative for energy supply.

1.1. Photovoltaic Water Pumping

In this context, various studies are conducted in the field of solar photovoltaic water pumping systems all around the world. For instance, a photovoltaic solar electrification system for a rural home was studied by Bhayo et al. [5]. A bank of batteries was used for the days with low irradiations or overnight. A specific uneven electricity consumption

profile was considered. It was shown that there are times with a surplus of energy, and this excess energy is used for pumping water. In addition to sizing and other technical aspects of the project, they also evaluated the levelized cost of energy of the system as an economic parameter. In another study by Vishnupriyan et al. [6], the variation of the tilt angle effects on electricity production, the efficiency of the system, and energy loss were investigated. The study was numerically conducted with PVsys software, and the best tilt angle of the system was determined. Tiwari et al. [7] studied solar water pumping by using MATLAB. To evaluate the performance of the system, different parameters of the pump head, PV panel configuration, and radiation were considered. They also studied optimized performance and sizing of the system. Raza et al. [8] investigated the social-economical-environmental impacts of using a photovoltaic-based high-efficiency irrigation system in Punjab, Pakistan. Half of the rural community relies on agriculture for a living and the energy crisis in Pakistan has adverse effects on people's lives. The results of the study showed that more people adopted high-efficiency irrigation systems, and this led to lower operational costs compared to conventional fossil-based systems, and consequently led to up to a 100% increase in farmers' net income. Furthermore, it was shown that more than 17 kilo tons of CO_2 emissions reduction per year, and 41% of water savings happened. In another study in Quetta city, Pakistan [9], the effect of running water wells with a photovoltaic water pumping system on the water table and discharge of its valley aquifer was investigated. RETScreen software was used to perform a financial cost-benefit analysis. The results led to recommendations for using two lower-capacity pumps for shallow wells and one higher-capacity pump for deeper wells.

1.2. The Concept of Water Shortage Probability (WSP)

In a study by Gualteros and Rousse [3], an open-access software was developed that assists in different aspects of pre-feasibility study, sizing, and optimization as well as maintenance and financial evaluations. The goal of the study was to help people with limited awareness about photovoltaic solar water pumping systems in off-grid rural areas. The concept of water shortage probability was introduced, as a special case of the loss of power supply probability, to establish water shortage tolerance of the community, and it was shown that the tolerance in water shortage has a considerable effect on the size and price of the system. In another investigation by Lunel and Rousse [10], a Python code was developed with the aim of solving the problem of expensive and less available for poor communities of commercial packages such as PVsyst or hard-to-handle tools such as the online tool, SISIFO. Their package is open source with the scope of modeling and sizing small solar photovoltaic water pumping systems for rural communities.

1.3. Photovoltaic Electricity in Iran

Despite having immense potential, a clean renewable energy industry is not yet well-developed in Iran. The reluctance to use renewable energy has been due to the low price of energy carriers in this country. However, nowadays this trend is changing. The change in Iran's policy toward renewable energy can mainly be attributed to unstable energy prices, the necessity for greenhouse gas emissions reduction, the creation of job opportunities, and relief from international sanctions [11]. The government has implemented incentive policies to use and invest in renewable energy. For example, the minister of energy of Iran has announced guaranteed purchase prices (feed-in-tariffs) for renewable electricity. This includes diverse types of renewable energy including solar PV, biomass, hydropower, geothermal, wind, and so on [12].

In 2016, Iran's agriculture industry consumed more than 36 GWh of electricity which represent more than 15% of the country's total power consumption [13], and it still has about 14–15% of the country's power consumption in 2020 [14]. In a study by Nikzad et al. [13], a solar water pumping system for irrigation of rice paddies in a northern province of Iran, i.e., Mazandaran, was investigated. The authors conducted both a technical and economic study, while the environmental aspects were investigated as well. Noise and CO_2 emissions were

complementary to the environmental parameters of their study. To enhance the reliability of the system, backup battery banks were considered. The idea of selling electricity in non-irrigation months of the year was then considered. The economic and environmental advantages of replacing a conventional diesel pump with a photovoltaic water pumping system were discussed. In another study by Niajalili et al. [15], the feasibility of a solar water pumping system in the northern province of Gilan was investigated for a typical rice paddy. Sizing of PV panels, as well as a comparison of the lifecycle cost of the solar water pumping system with that of the conventional ones were performed. It was shown that the initial cost of the solar water pumping system could be up to nine times that of a conventional system. However, the total lifecycle cost of this solar system is in turn about 33% lower than its conventional counterpart. In a numerical study by Shahverdi et al. [16], a parabolic trough collector was considered as the heat source for an organic Rankine cycle. The cycle was designed for a pressurized irrigation system and eight different organic fluids were tested. The cycle produced the required electricity for the water pumping system. It was shown that the maximum efficiency of the Rankine cycle was 12.19%, with 47.85% of corresponding collector efficiency. In another study, a comparative financial investigation was conducted by Parvaresh Rizi et al. [17] for pressurized irrigation water pumping systems with both conventional (fuel and on-grid) and solar systems. The study revealed that in general, when the required pumping power is more than 3 kW and the transmission electricity line is less than 2 km, it is more affordable to supply the required energy from a private power transmission line. The authors mentioned that Iran is highly dependent upon its subsidized fossil fuels and that new policies are required to finance solar water pumping projects. Chahartaghi and Nikzad [18] studied energy, exergy, and greenhouse gas emission reduction of a photovoltaic water pumping system for a potato farm in Isfahan, Iran, at different ambient temperatures and irradiations. The minimum and maximum exergy efficiency of the PVWPS was shown to be 0.27 and 3.56%, respectively. The proposed system could avoid the emissions of 4.8 tons of CO_2 annually which is equal to 11.1 barrels of crude oil.

1.4. Aim of This Study

In the context of this specific review, the goal of this study is to investigate the techno-economic parameters of a small-scale PV-battery solar electrification and water pumping system for a typical citrus farm located in the Hormozgan province of Iran by considering the LPSP and WSP concepts. It is aimed to show how selecting appropriate (or tolerable) values of LPSP and WSP can affect the overall cost of the system and thus show that the capital cost (CAPEX) and LCOE totally depend on the user's threshold selected for these two parameters. In fact, the original idea is to link the performance of the system in terms of CAPEX and LCOE to the concepts of WSP and LPSP tolerances by a population when it comes to proposing systems that provide both electricity and water. Initially, the optimum fixed tilt angle of the PV panels is determined. Based on the profile of the crop's water requirements in different months and the corresponding electricity load, the sizing of PV panels and the battery bank backup system is performed to enhance the reliability of the system.

1.5. Principal Contributions of This Study

Several preponderantly interesting results were found here:

1. A comparison of different LPSPs shows that a small increase in tolerance for power loss can considerably lower the size, the CAPEX, and the LCOE of the system with limited change in water shortage probabilities. This suggests that communities and/or dwellings with limited financial capabilities should consider complementary strategies to avoid running out of water for irrigation.
2. The WSP could go lower with higher LPSP because more water could be pumped into the tank when people can tolerate power shortages.

3. There is a minimum in the curve that plots the CAPEX with respect to the number of PV panels in the system where limited variations of WSP and LCOE happen with further increases in the number of PV panels and that for any LPSP. This is due to the battery bank requirement rapid increase below the minimal number of panels which are less expensive. For the current study, this is about 5 to 6 panels.
4. Overall, the main findings are that the success of a project will depend on the resilience of the population combined with its financial capacity.

2. Methodology

In this section, only the preponderant elements of mathematical modeling along with the schematic of the investigated system are outlined to avoid making the paper overly lengthy. Afterward, in Section 2.2, the specific configuration of the benchmark problem used for the validation is depicted. In Section 2.3, the genuine algorithm used to simulate the problem is depicted and briefly discussed. Then, specifications of the main components of the system are provided in Section 2.4 in the form of tables and validation is provided against a specific benchmark problem. Finally, the case study is investigated, and it involves the same components used in the benchmark reference. It is worth specifying that the rationale behind the choices embedded in Sections 2.2 and 2.4 come from the need to validate the whole model against results available in the literature, according to the study of Bhayo et al. [5]. A different topology could be implemented, and different components could be used in further studies.

2.1. Mathematical Modeling

In order to estimate the total amount of solar irradiation on a tilted surface, the hourly values of global horizontal, direct normal, and diffuse horizontal irradiance should be used. Data provided by the National Solar Radiation Database (NSRDB) [19] for Indian Ocean Data Coverage (IODC) by the Meteosat satellite with Physical Solar Model Version 3 (PSM-v3) are used in this study. Currently, it provides mean Direct Normal irradiation (DNI) for the years 2017–2019. The values for the last available year i.e., 2019 are considered herein. It is worth noting that using average values for these years could be questionable since averaging eliminates the extrema in irradiance. This can negatively affect the reliability and accuracy of system sizing. Of course, selecting a particular year involves limitations too, but it reduces the possibility of underpredicting required capacity.

2.1.1. Basic Solar Mathematical Model

To obtain an estimate of the total amount of energy that strikes a surface with a given slope and orientation, one needs to determine and calculate several variables, mainly times and angles, hereafter defined in the nomenclature.

Most of the material presented in this section is based on the classical textbook by Duffie and Beckman [20]. The basic concepts are provided with the aim of recalling the main steps which make it possible to determine the angle of incidence of direct radiation on a surface necessary to obtain the irradiance. First, the declination angle of the sun is obtained with [21,22]:

$$\Delta = 23.45 \times \sin\left(360 \times \frac{284 + n}{365}\right) \tag{1}$$

where n is the number of the current day starting from the first of January (n = 1) to the 31 December (n = 365). The sunset hour angle is [20]:

$$\omega_{SS} = \arccos\left(-\tan(\varphi) \times \tan(\delta)\right) \tag{2}$$

where φ is the latitude of the city under study. Sunrise hour angle, ω_{sr} equals $-\omega_{ss}$. Sunrise and sunset hour angle are used to calculate sunrise and sunset. The hour angle is defined as:

$$\omega = 15 \times (12 - ST) \tag{3}$$

where ST is solar time obtained with:

$$ST = LT + \frac{(EOT + 4 \times (LL - LSTM))}{60} \tag{4}$$

where LT is local time, EOT is the equation of time, LL is local longitude, and LSTM is the local standard time meridian. For LSTM, 15 degrees should be multiplied by the difference from Greenwich time. EOT is obtained from:

$$EOT = 9.87 \times \sin(2 \times \Gamma) - 7.53 \times \cos(\Gamma) - 1.5 \times \sin(\Gamma) \tag{5}$$

$$\Gamma = 360 \times \frac{(n - 81)}{365} \tag{6}$$

The zenith angle θ_z is defined as [20]:

$$\theta_Z = \text{arc} \cos(\sin(\delta) \times \sin(\varphi) + \cos(\delta) \times \cos(\varphi) \times \cos(\omega)) \tag{7}$$

And finally, the required angle of incidence is defined as [20]:

$$\theta = \text{arc} \cos(A + B + C) \tag{8}$$

where:

$$A = (\sin(\varphi) \times \cos(\beta) - \cos(\varphi) \times \sin(\beta) \times \cos(\gamma)) \times \sin(\delta) \tag{9}$$

$$B = (\cos(\varphi) \times \cos(\beta) + \sin(\varphi) \times \sin(\beta) \times \cos(\gamma)) \times \cos(\delta) \times \cos(\omega) \tag{10}$$

$$C = \cos(\delta) \times \sin(\beta) \times \sin(\gamma) \times \sin(\omega) \tag{11}$$

In Equations (7)–(11), φ, δ, β, γ, and ω are the latitude of the location, the declination angle, the tilt and azimuth angles of the surface, and the hour angle, respectively. Hourly global solar radiation on an inclined surface is composed of three terms: direct beam, diffuse, and ground reflected radiation [20]:

$$I_\beta = I_b R_b + I_d \frac{1 + cos(\beta)}{2} + I \times \mu \times \frac{1 - cos(\beta)}{2} \tag{12}$$

where I_b, R_b, I_d, I, and μ are the direct beam radiation, a geometric factor, the diffusive radiation, the global horizontal radiation, and the albedo coefficient, respectively. R_b is defined as [20]:

$$R_b = \frac{cos(\theta)}{cos(\theta_z)} \tag{13}$$

It is worth noting that $R_b = 0$ between sunset and sunrise.

2.1.2. Electricity Production Model

In order to obtain the output power of the PV panel, Equations (14)–(16) are used [5,22,23]:

$$P_{PV}(t) = N_{PV} \times I_{PV}(t) \times V_{PV} \tag{14}$$

where N_{pv} and V_{PV} are the number and voltage of the panels. I_{PV}, the current of the panel is:

$$I_{PV}(t) = I_{PV,r} \times \left(\frac{G(t)}{G_{STC}}\right) \times (1 + \alpha \times (T_C(t) - T_{C,STC})) \tag{15}$$

$I_{PV,r}$ is the panel's rated current, and G(t) is the surface incident solar irradiation. Similarly, G_{STC} is incident solar irradiation on the surface on standard test conditions, and α is the temperature coefficient. Furthermore, T_C is the temperature of the panel, and it

increases as the incident irradiation on the surface increases. $T_{C,STC}$ is the temperature of the cell under standard test conditions. The following equation is utilized to consider the effect of irradiation of temperature:

$$T_C(t) = T_{amb} + \left(\left(\frac{NOCT - 20}{800} \right) \times G(t) \right) \tag{16}$$

NOCT is the nominal operating cell temperature. It is worth noting that T_{amb} is the ambient temperature, and it is available for each hour of the year. The charging and discharging states of the batteries are calculated through the following equations, respectively [23]:

$$SOC_{Charging}(t) = SOC(t-1) \times (1 - \sigma) + \left(P_{PV}(t) - \left(\frac{P_l(t)}{\eta_{inv}} \right) \right) \times \eta_{bc} \tag{17}$$

$$SOC_{Disharging}(t) = SOC(t-1) \times (1 - \sigma) - \frac{\left(\left(\frac{P_l(t)}{\eta_{inv}} \right) - P_{PV}(t) \right)}{\eta_{bd}} \tag{18}$$

where σ is the hourly self-discharge rate, and Pl denotes load power. Furthermore, η_{bc} and η_{bd} represent the efficiency of the battery at charge and discharge mode, respectively. Values of σ, η_{bc}, and η_{bd} are 0, 0.97, and 1, respectively [5,24]. Finally, to complete the model, η_{inv} is the efficiency of the inverter.

2.1.3. Water Pumping Model

Now, when it comes to simulating pumping, one needs to calculate π, the pumping power of the system. The following equation is then used [5]:

$$\pi = \rho \times g \times \dot{V} \times vH \tag{19}$$

where ρ, g, $\dot{V}$, and H are the density of water, gravitational acceleration, volumetric flow rate, and total dynamic head. In the following simulations, the total head of the pumping system is set to be 8 m to allow a direct comparison with the benchmark study. The efficiency of the pump is considered 90%, which should be taken into consideration in Equation (19).

2.1.4. Reliability Models for Power and Water

In order to assess the reliability of the system, two terms, LPSP and WSP, are considered. LPSP is defined as:

$$\text{LPSP } (\%) = \frac{\sum_{t=1}^{t=8760} LPS(t)}{\sum_{t=1}^{t=8760} P_l(t)} \times 100 \tag{20}$$

where LPS(t) is loss of power supply at time t and is considered as the difference of demand and supply at that instance of time. WSP can be considered a special case of LPSP. It is then defined as:

$$\text{WSP } (\%) = \frac{\sum_{d=1}^{d=365} WS(d)}{\sum_{d=1}^{d=365} IWR(d)} \times 100 \tag{21}$$

It is worth noting that WS(d) is the deficiency of water on day d, which analogously accounts for the difference in water supply and water demand on that specific day. The selection of hours or days for the definition of WSP is based on the required precision of the system. Since the hourly definition of WSP is strict and unnecessary, it is considered based on its daily definition.

2.1.5. Financial Model

For the financial analysis, the levelized cost of energy (LCOE) is investigated. LCOE shows the unit price of energy per kWh by applying the current value of total cost over the project's lifetime [5]. The general form of LCOE is then given by:

$$\text{LCOE} = \text{Life Cycle Cost}/\text{Lifetime Energy Production} \tag{22}$$

The simplified discounting form of LCOE is used in this study, as described in [5]:

$$\text{LCOE}_{\text{Discounting}} = \frac{CAPEX_0 + OPEX_t}{\sum_{t=0}^{Lifetime}\left(\frac{EP_t}{(1+r)^t}\right)} \tag{23}$$

where EP_t is electricity production in year t and r is the real discount rate that is considered 15% [13]. $CAPEX_0$ and $OPEX_t$ are the investment or capital expenditure of components and total operational annual expenditures, respectively.

The total capital expenditure involves the PV, pump, and other parts of the system such that:

$$CAPEX_0 = CAPEX_{0-PV} + CAPEX_{0-pump} + CAPEX_{0-else} \tag{24}$$

while $OPEX_t$ is obtained from the following equation [5]:

$$OPEX_t = O_t + M_t + R_t + F_t \tag{25}$$

where O_t, M_t, R_t, and F_t are operational, maintenance, replacement, and fuel costs, respectively. The operational cost is assumed to be zero as there is no need to "operate" anything [5]. The maintenance cost M_t is assumed to be two percent of the PV and pumping investment costs [5,25], as in Equation (26). In this study, only PV-system-related costs, pumps, and storage-related costs are accounted for in M_t. The salvage values of the components are neglected because they are assumed to be used over their lifetime [26–28]. The other related capital expenditures + $CAPEX_{0-else}$ are assumed to imply no maintenance. Therefore:

$$M_t = 0.02 \times CAPEX_0 = 0.02 \times [CAPEX_{0-pv} + CAPEX_{0-pump}] \tag{26}$$

In the present study, the PV system unit capital cost is assumed to be 0.93 $/W [5], which includes 40 percent of the installation costs. At the same time, the pump storage system is considered to have a unit capital cost of 2.4 $/W [29–31].

The Lifetime of the project is fixed at 30 years. It is also assumed that the annual electricity yield EP_t will be constant every year during the project's lifetime and that there is no output energy degradation during the lifetime of the project. Based on the life span of components, the replacement cost is defined as:

$$R_t = R_{battery} + R_{inverter} \tag{27}$$

$$R_{battery} = CAPEX_{0-battery} \times \left(\frac{1}{(1+r)^5} + \frac{1}{(1+r)^{10}} + \frac{1}{(1+r)^{15}} + \frac{1}{(1+r)^{20}} + \frac{1}{(1+r)^{25}}\right) \tag{28}$$

$$R_{inverter} = CAPEX_{0-inverter} \times \left(\frac{1}{(1+r)^{10}} + \frac{1}{(1+r)^{20}}\right) \tag{29}$$

Here F_t equals zero as transportation in internal combustion engine's vehicles and other fossil fuel-based maintenance costs are embedded in M_t.

2.2. Schematic of the Solar Irrigation System

The schematic of the solar irrigation system is depicted in Figure 1. The DC electricity produced by the PV Array is converted to AC through a solar Inverter, and it is conducted

to a Switch Board that supplies either the Residence Load or a Bi-directional Inverter. This Bi-directional Inverter is responsible for both Battery Bank charging/discharging and supplying electricity to the Motor-Pump which in turn fills the Water Tank of the pumping system enabling irrigation of the Farm.
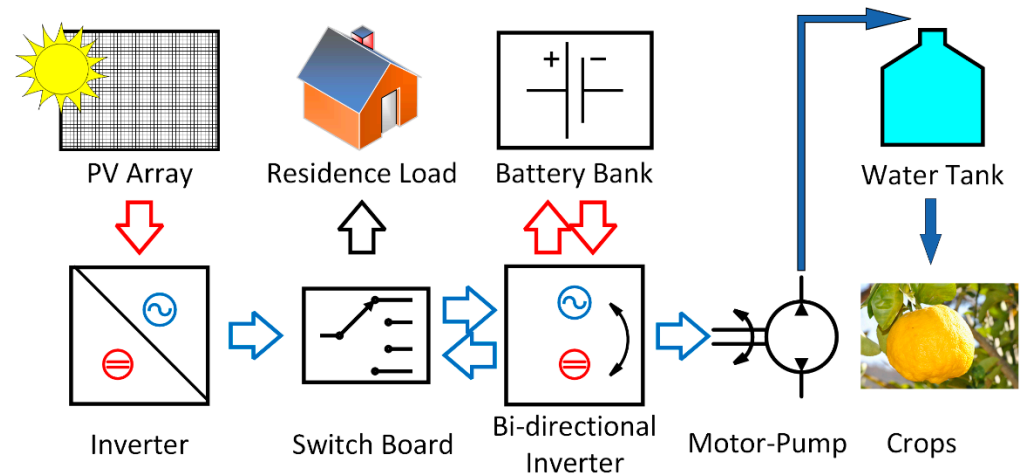

Figure 1. Schematic of the water pumping system with DC/AC conversion directly after the PV panels.

Figure 1 clearly indicates that an inverter is inserted between a switchboard and the PV array itself, thus readily converting DC to AC. A different choice could be made, according to the pump type (AC or DC), for instance. However, the justification for this choice stems from the requirements for validating the formulation and implementation of the model, which is then validated against the model proposed in [5]. This configuration is also used for the simulation discussed in Section 3 without loss of generality.

2.3. Algorithm of the Prediction Model

Figure 2 shows the first part of the algorithm of the prediction model for the system. In brief, the system mandates when to charge the batteries, when to supply electricity to the residents, and finally, when to run the pump depending on the availability of sun and the state of charge of the batteries. First, inputs such as GHI, DHI, DNI, ambient temperature, longitude, latitude, etc. are used to calculate total irradiation on the tilted surface. Then, the maximum annual total irradiation on titled surfaces is calculated, and the angle relevant to the maximum value is selected for investigations. Subsequently, global tilted irradiation, power load profile, irrigation water requirement, specification of components, and an initial PV array size are computed, and an initial value for system size are considered for calculations of PV power output.

Figure 3 shows the iterative procedure. The algorithm verifies whether or not the PV power generation matches the load at a given time. On the one hand, when the available power is higher than the load, then the algorithm verifies the SOC of the batteries: when the battery pack is not fully charged, priority is given to charging; when the battery pack is full, the pump starts and fills the reservoir. On the other hand, when the load exceeds the PV power, then the algorithm still verifies the SOC of the batteries: when the battery pack SOC is lower than SOC_{min}, the algorithm goes back to increasing the size of the battery pack and other relevant components (B in Figures 2 and 3). Hence, the algorithm calculates water pumping values, SOC for charging or discharging states, and ultimately the LPSP. When the LPSP tolerance is met, the sizing is favorable and the LCOE, CAPEX, and WSP are calculated; when the LPSP is higher than the maximum allowed $LPSP_{max}$, the loop recalculates the above-mentioned parameters by increasing the size of the battery and other components in order to reach the favorable LPSP (B in Figures 2 and 3). It is worth noting

that the program is repeated for N_PV$_{max}$ of 1 until the maximum number of PV panels which is considered by the user (C in Figures 2 and 3).
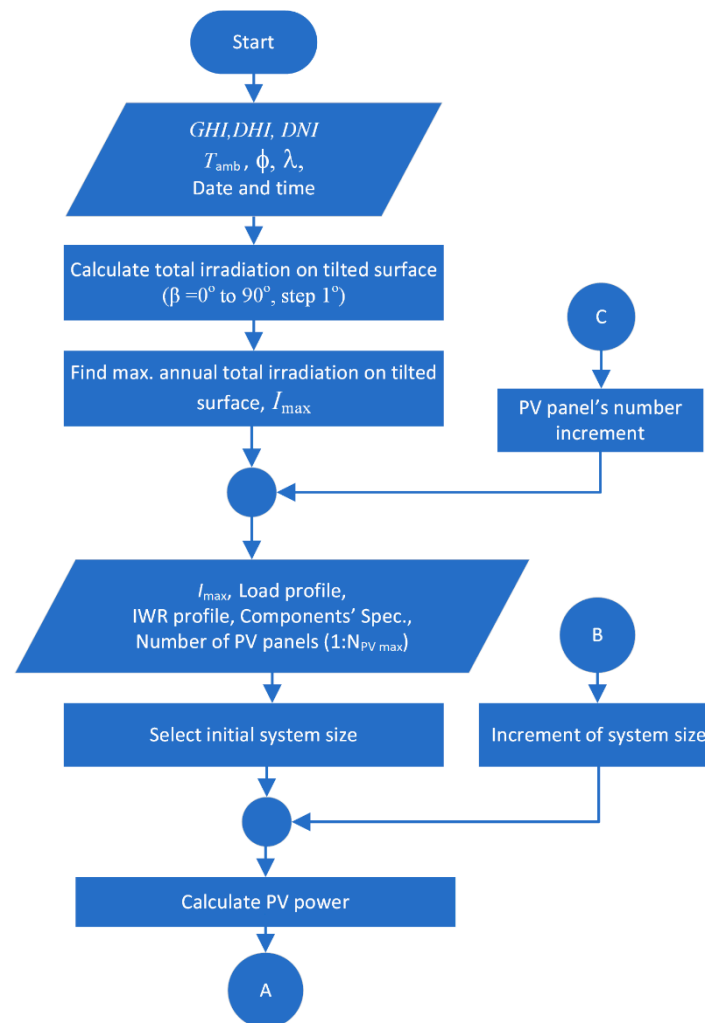

Figure 2. The first part of the algorithm of the study: the upper part computes the maximum irradiation on a tilted surface for the relevant location and the lower part introduces the user and system needs and provides an initial number of panels. Then, it selects an initial system size and computes the hourly total amount of power production in a year.

2.4. Specification of Components

The specifications of all components including PV panel, battery, solar inverter, Bi-directional inverter, and pumping storage system are succinctly shown in Tables 1–5. These components were chosen in order to benchmark outcoming predictions with respect to the relevant study of Bhayo, Kayem, and Gilani [5]. It is worth noting that for a better life expectancy for batteries, their minimum and maximum SOC are considered as 35 and 90% of their maximum capacity, respectively. The lifespan of batteries is five years. After that period, they are considered to have no residual value and hence no salvage value. On the other hand, the inverters are assumed to work for 10 years although they could last longer. The panels are considered to work for the whole duration of the project, i.e., 30 years, without loss of performance, which could be interpreted as a strong assumption.
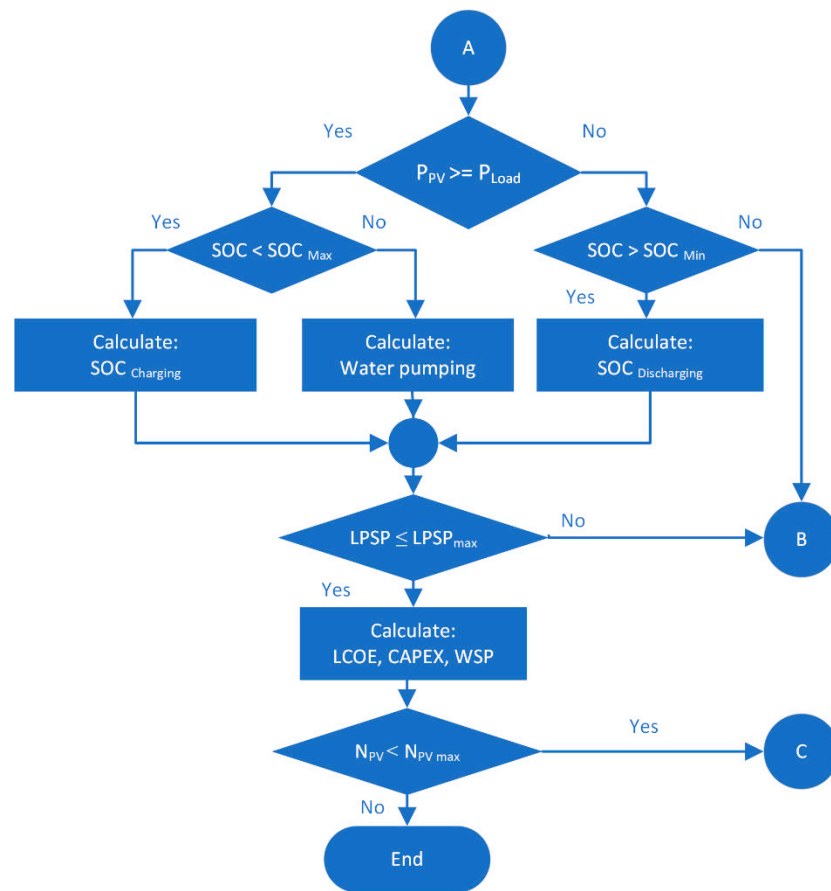
Figure 3. The second part of the algorithm: when $P_{PV} \geq P_{Load}$, the system first charges the batteries and then fills the reservoir; when $P_{PV} \leq P_{Load}$, the system calculates the discharging rate of the battery up to SOC_{min}. If this threshold is reached, the loop recalculates the above-mentioned parameters by increasing the size of the battery and other components.

Table 1. PV panel specifications [5].

PV Model	CS3K-305MS
Type	Monocrystalline
Power at STC, P_{mp}	305 W
Optimum operating Voltage at STC	32.7 V
Optimum operating Current at STC	9.33 A
Module Efficiency	18.36%
Temperature Coefficient (α)	-0.37% per °C
Nominal Module Operating Temperature	42 °C
PV life span	30 Years
Price	201.31 $

Table 2. Battery specifications [5].

Battery Model	8A31DT-DEKA
Battery Technology	Absorbent Glass Mat.
Nominal Voltages	12 V
Battery Capacity	104.0 Ah
Battery life span	5 years
Depth of discharge	60%
Price	362.25 $

Table 3. Solar inverter specifications [5].

Model	SMA Sunny Boy 2.0
Continuous AC Output Power	2000 W
Min/Max Input DC Voltages	80/600 V
Max Input DC Current per string	10 A
Max. short circuit current per string	18 A
Power consumption while operating	2 W
Efficiency	97%
Life span	10 years
Price	867 $

Table 4. Bi-directional inverter specifications [5].

Model	Multi-Grid
Type	VDE-AR-N 4105
Power Output from 25 °C to 40 °C	2400 to 2200 W
Maximum efficiency	94%
Rated Input Voltage DC/AC	19–33/187–265 V
Rated Output Voltage DC/AC	24/230 V
Rated Output DC	70 A
Life span	10 years
Unit Price	992 $

Table 5. Pumping and storage system specifications [5].

Yearly Operation and Maintenance Cost	2% of Investment Cost
Pump Efficiency	90%
Total head	8 m
Life span	30 years
Investment cost	2.4 $/W

2.5. Validation

To validate the correct formulation and implementation of the proposed genuine algorithm, the results are tested against those found in reference [5]. In this study, Bhayo, Kayem, and Gilani use a site located in Malaysia, and hence for the validation process, the same site with the same demand is used, but here, of course, the genuine part of the algorithm (the bottom part) is not explicitly employed.

First, in Figure 4, the installed battery capacity (IBC) in Wh, the daily average power generation in kWh/day, and the water pumped to provide storage in m^3/day are presented as a function of the number of PV panels installed in the installation. In Figure 4, as the number of PV panels increases, the required capacity of the battery decreases. This is due to the fact that the battery is supposed to compensate for the lack of energy supply. As the PV panel capacity increases, less electricity deficiency happens, leading to more system reliability; hence less battery capacity is required. On the other hand, an increase in PV panel number leads to more power generation during the lifetime of the project and more water pumping. In Figure 4, the current predictions are found to accurately reproduce the results proposed in the benchmark publication.
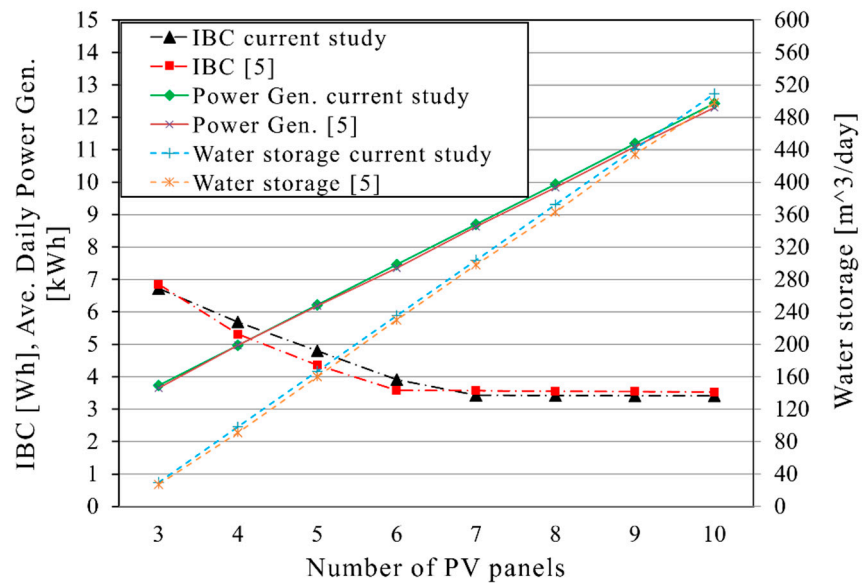
Figure 4. Validation of technical results of the current study with Reference [5].

Figure 5 presents the lifetime power generation of the system in kWh, the lifetime cost in $, and the LCOE in $/kWh. It shows that increasing the number of PV panels makes the LCOE decrease, especially below seven panels. This is because as the number of PV panels increases, more power is produced during the lifetime of the project and because the first increase in the number of panels does not affect the lifetime cost too much. Based on the definition of LCOE (Equation (22)), the cumulated generated power is the denominator of LCOE, while the cost is the numerator. Then, as increasing PV panels above six leads to an increment of the lifetime cost of the system (or the numerator of Equation (23)) simultaneously with the denominator, Figure 5 indicates a more or less stabilization of the LCOE above seven panels for this specific simulation. Here again, the agreement with the predictions found in [5] for the same problems is excellent.
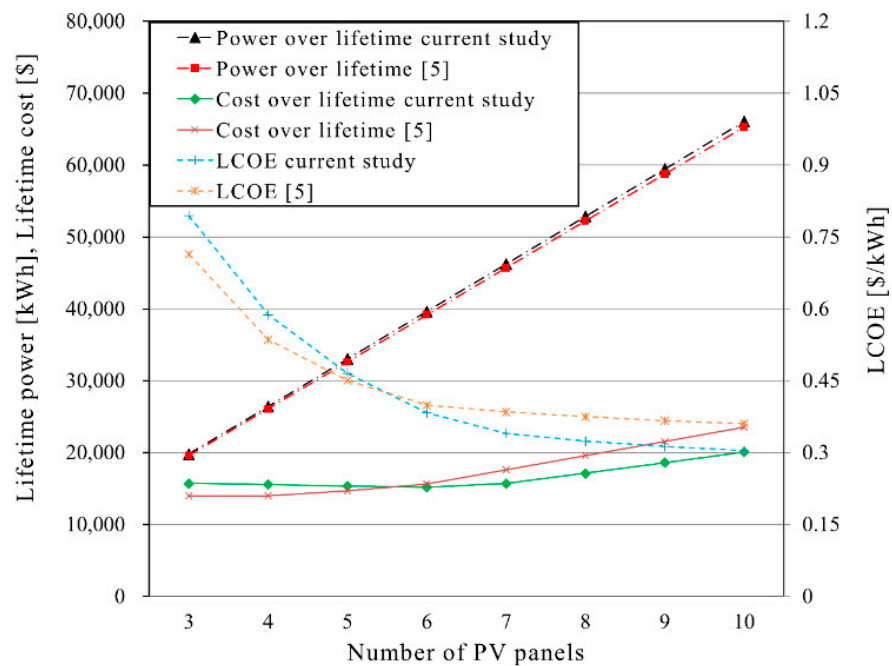
Figure 5. Validation of economic results of the current study with reference [5].

The above results provide confidence in the ability of the proposed model to simulate the citrus farm of Bandar-Abbas presented next.

2.6. Case Study

Iran has a great potential for solar energy use especially in central and southern parts of the country [32,33], Figure 6. The capital of Hormozgan province, i.e., Bandar Abbas is considered for investigation. This city has a latitude and longitude of 27.17 degrees North and 56.26 degrees East, respectively.
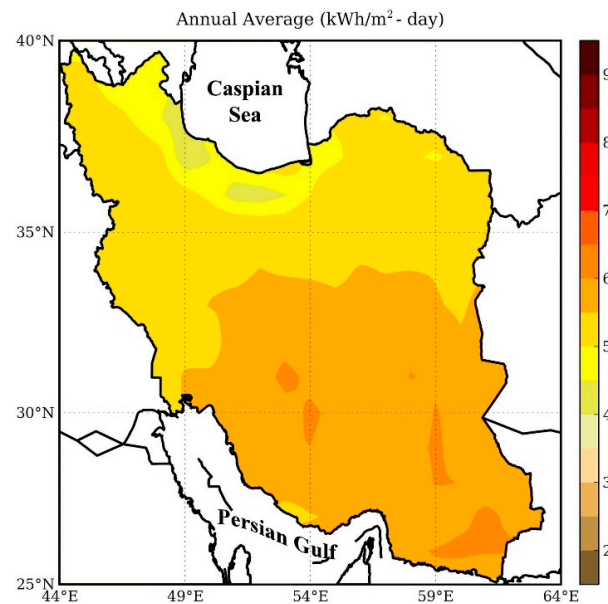

Figure 6. Total radiation on a fixed south-facing surface with a tilt angle equal to latitude [32,33].

The amount of daily average global horizontal insolation as well as the ambient temperature for Bandar Abbas for each month of the year is shown in Figure 7. From April to the end of September, the average daily insolation on a horizontal surface is above 5 kWh/m^2 while the ambient temperature is above 25 °C. On the one hand, the higher the irradiation, the better the electricity production. On the other hand, ambient temperatures above 25 °C will necessarily lead to lower cell efficiencies as the surface temperatures will impair production. The maximum daily average is 6.5 kWh/m^2 in June, while the maximum average temperature reaches 36 °C in June, July, and August.
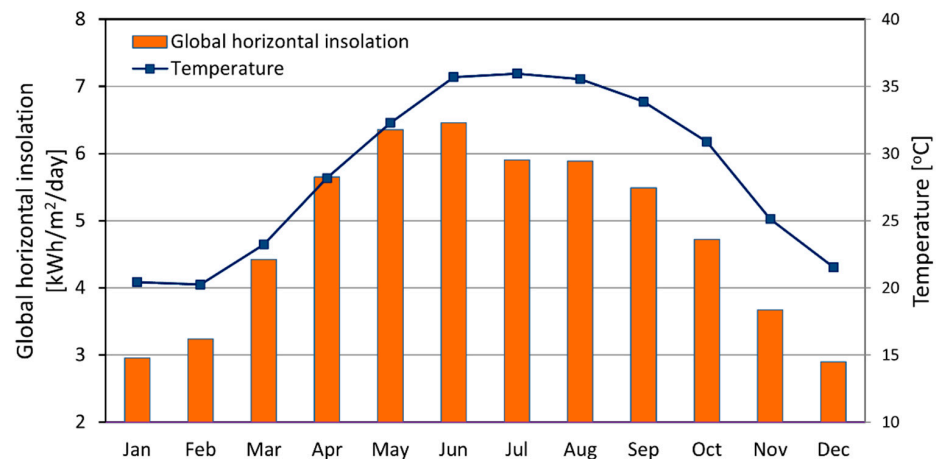

Figure 7. Monthly average Global horizontal insolation as well as ambient temperature for Bandar Abbas.

The hourly diagram of the global horizontal irradiation for one year is very noisy, as evidenced by the profile depicted in Figure 8, produced from the NSRDB data set [19]. Calculations are based on this profile. In Figure 8, sudden drops in GHI values mainly correspond to clouds and/or rainy periods.
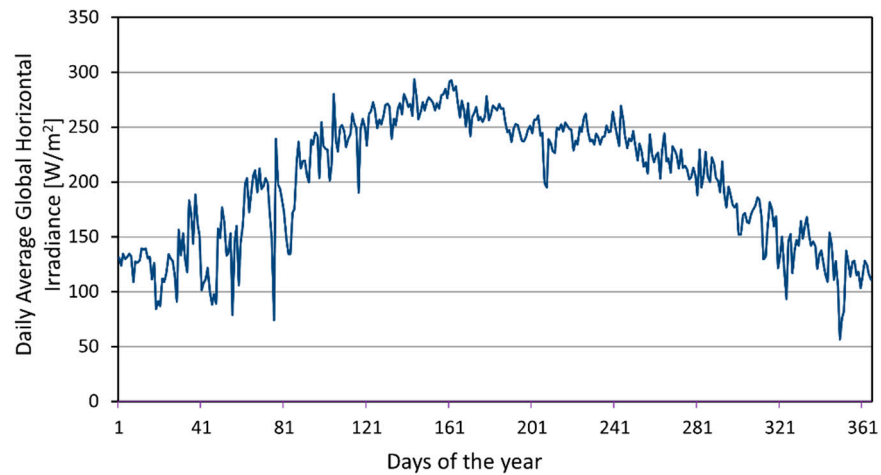

Figure 8. Daily average global horizontal irradiance (GHI) for Bandar Abbas.

Irrigation water requirement (IWR) and crop water requirement (CWR) are terms mostly used in agricultural water management topics. IWR is the net depth of water needed for a crop to satisfy its water requirement (in mm). In fact, IWR is the fraction of CWR not supplied through rainfall, groundwater, and storage of water in soil [34]. Figure 9 depicts IWR and CWR for citrus farms at Hormozgan provincial level [35]. To obtain an average daily irrigation water requirement, a trendline is fitted with a polynomial regression of order 6. The equation is:

$$IWR = -0.0091 \times m^6 + 0.3545 \times m^5 - 5.1071 \times m^4 + 32.086 \times m^3 - 81.701 \times m^2 + 91.436 \times m - 4.4536 \qquad (30)$$

where m is the month number. Here, order six ensures that $R^2 = 0.9948$. The unit for IWR is mm and it should be multiplied by the area of the farm (1 hectare) to obtain the total volume of water required for irrigation.
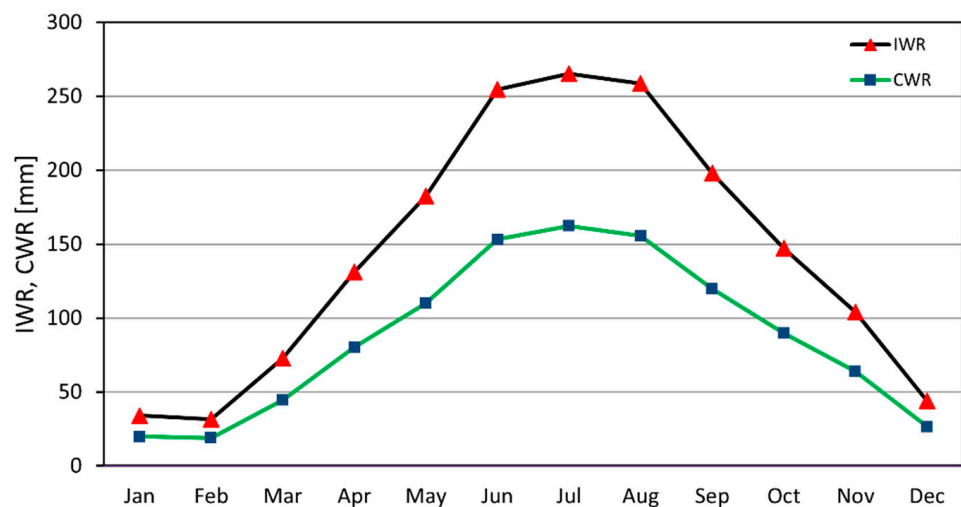

Figure 9. Irrigation and crop water requirement for a citrus farm in Hormozgan province [35].

To complete the description of the total electrical load of a typical installation, the hourly average electricity load for a typical house, constructed from several different profiles, is depicted in Figure 10. In the proposed profile, reasonable increases in electricity demand, with respect to the basic load, are considered for the morning (from 6 to 8), noon (from 13 to 14), and night (from 19 to 23). The profile also shows a 50% increase in the basic 100 W load between the afternoon peaks (from 15 to 18). It is worth mentioning that different shapes can be used as load profiles based on appliance users' profiles, as long as they reflect a reasonable pattern for a residential house.
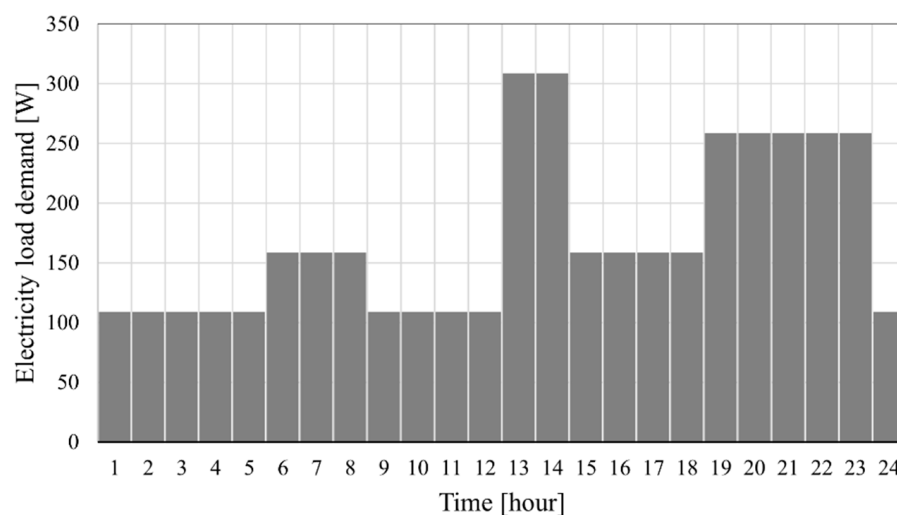
Figure 10. Hourly electricity load for a typical rural house.

3. Results and Discussions

In this section, the results obtained in an attempt to optimize a citrus farm located in Bandar-Abbas in terms of LCOE, CAPEX, and WSP for three different LPSPs are presented.

The first concern is to determine the most suitable fixed tilt angle for the PV array (oriented due South). Despite simple rules of thumb considerations for the best PV tilt angle, the problem of panel slope for yielding the maximum solar energy collection can be complex and it is a function of various parameters such as local latitude, surface azimuth, and clearness index [36]. The variation of the yearly average daily irradiation with respect to the slope of the array was calculated for $0 \leq \beta \leq 90°$. The optimal tilt angle that leads to the maximum power generation of PV panels for one year is about $\beta = 17°$ for this city. These results for the optimum tilt angle were confirmed with respect to the cumulative electricity production in a year (not explicitly presented). It is worth mentioning that, although the maximum value of average daily irradiation occurs at $17°$, limited reductions were found in the range of 10 to 28 degrees. Therefore, construction of the structures (not considered herein) could be much easier at $20°$, for instance, without substantial losses in performance.

In Figures 11–14 the results of the study in terms of the variations of WSP, LCOE, and CAPEX with respect to the number of PV panels are presented for three different thresholds for LPSP. It is assumed that the residents need different reliabilities for their electricity demand leading to LPSP values of 0, 1%, and 3% in Figures 11–13, respectively. One should note that despite similar shapes, the y-axes of these figures involve different scales. The lower the value of LPSP, ceteris paribus, the higher the corresponding values of all three other parameters.
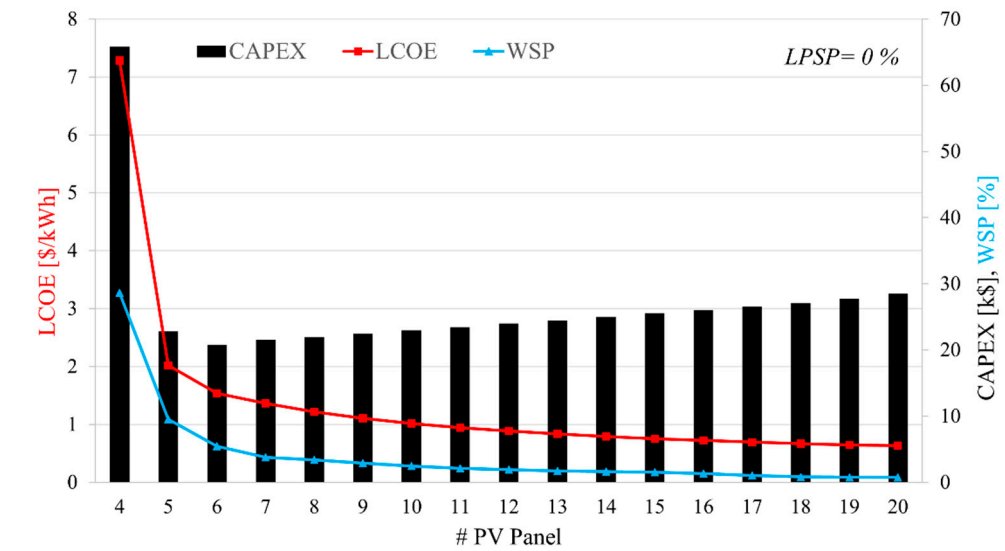
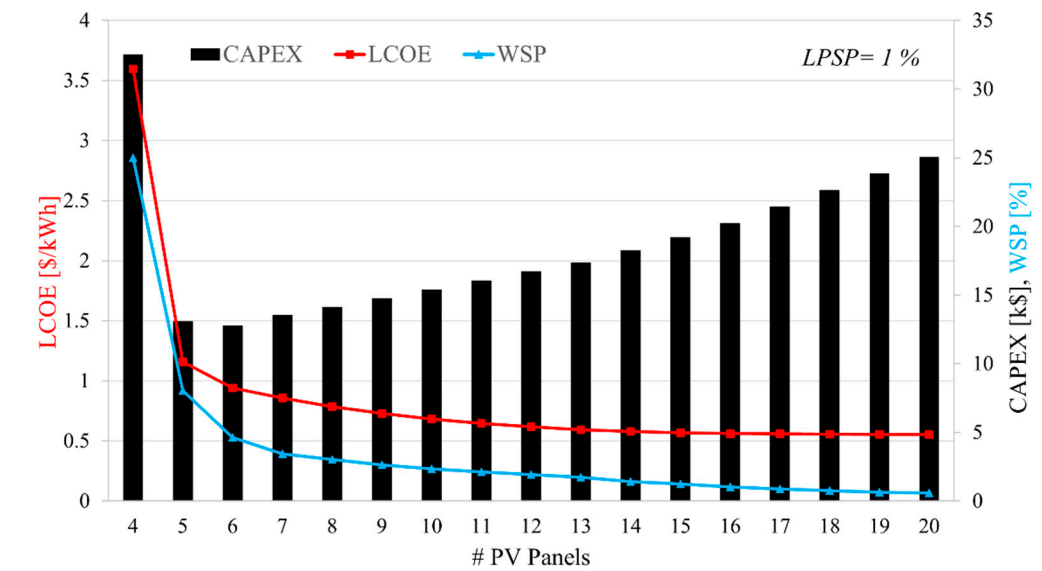**Figure 11.** The number of PV panels versus LCOE, CAPEX, and WSP for LPSP = 0%.

Figure 12. Number of PV panels versus LCOE, CAPEX, and WSP for LPSP = 1%.

In Figure 11, LPSP = 0 simply means 100% reliability of the system in providing electricity for the residence, 365 days per year. Therefore, based on the algorithm used in the study, LPSP is fixed to the desired value (or tolerance of a customer, or community), and the minimum PV panel and battery capacity are obtained accordingly. In Figure 11, the capital cost of a 4 panel system (left in Figure 11) reaches 66,000 $, while the WSP peaks at more than 28% and the LCOE exceeds 7 $/kWh as there is a major requirement for batteries. However, a slight increase in the number of panels produces a rapid decline in both the WSP and LCOE. Nevertheless, the symbolic threshold of 1 $/kWh reaches around 10 panels and further increases do not change the LCOE significantly while the CAPEX increases.

It is obvious that as the number of PV panels increases, the water shortage probability will decrease since the system is capable of producing more electricity. This is mostly at the expense of an increment in the capital cost of the project (CAPEX). Moreover, this is true for the three values of LPSP.
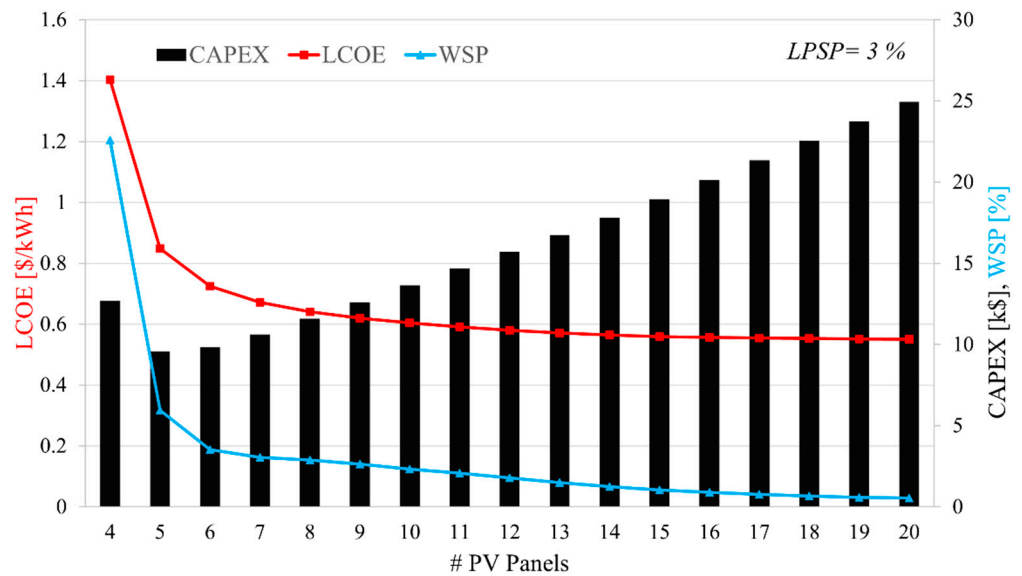
Figure 13. Number of PV panels versus LCOE, CAPEX, and WSP for LPSP = 3%.
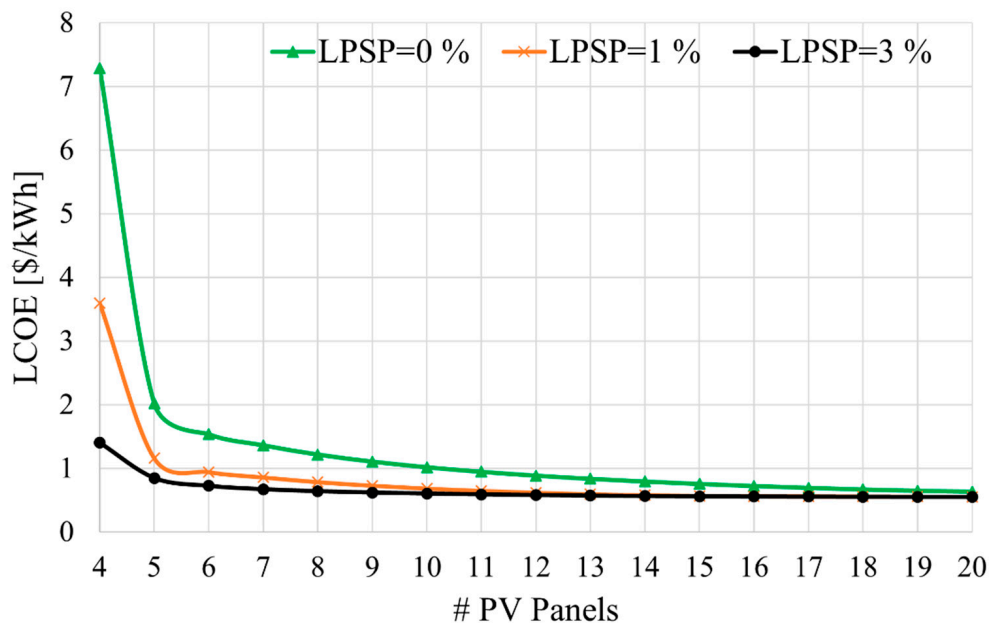

Figure 14. Comparison of different LCOE values for three LPSP tolerances of 0, 1%, and 3%.

In Figure 12, similar trends are observed. However, 10 panels with LPSP = 1% will lead to an LCOE of about 33% less than that calculated in Figure 11. Logically, a higher LPSP has an important effect on the capital cost. CAPEX drops from about 23,000 $ (Figure 11) to 15,000 $ (Figure 12) for a 10 panels system.

As the LPSP has such an influence, simulations were also carried out for a 3% LPSP and the results are reported in Figure 13. Here again, similar trends are observed. However, 10 panels with LPSP = 3% will lead to an LCOE drop of about 40% while the CAPEX reaches as low as 14,000 $ for the 10 panels system.

From Figures 11–13, it can be seen that there is a minimum value for the capital cost of the system at different LPSP values. This minimum value happens for 6, 6, and 5 PV panels and for LPSPs of 0, 1%, and 3%, respectively. This is due to the fact that generally, increasing PV panels means making the system bigger, and hence more investment is needed. However, as mentioned earlier, at the extremely low number of PV panels, considerable amounts of battery bank capacity are required for the system to guarantee the threshold

values for LPSPs, and consequently, in this case, the battery price dictates the high values of the CAPEX.

The variation of the systems capital cost at PV panel numbers of 4 to 5 or 6 is considerable in all cases of LPSPs. For LCOE trends, the same as the explanations provided in the previous section, i.e., validation section, LCOE decreases by increasing the number of PV panels, since the production of electricity is much higher than the increment in investment cost of the system.

At a fixed LPSP value, the selection of the best sizing of the system in terms of the number of PV panels and battery bank capacity depends on the tolerance of WSP and the capability of the user to pay the investment cost of the system. In fact, this is the end user who decides which system size is compatible with their needs. Here, it is worth noting that WSP = 1% means that there is a yearly average of about 3.6 days for which there could be a water shortage, not a guaranteed shortage. In these periods, the requirement for irrigation could also be less, thus modifying the water demand, as the WSP is correlated to irradiation. Nevertheless, several strategies could be considered to solve this problem, such as personal water storage by individuals during sunny days, prior to critical periods of the year, or variable prices of water per liter with weather predictions. Yet these strategies are not reviewed here.

For instance, Figure 14 shows that at LPSP = 0, for a PV panel number of five, the LCOE is about 2 $/kWh and reduces to about half at 10 PV panels and to 0.75 $ per kWh at 15 PV panels. This suggests that there should not be much gain in terms of LCOE to increase the number of panels above 10. Furthermore, at LPSP = 0, WSP values for these panel numbers are 9.5%, 2.4%, and 1.5%, respectively (Figure 15). This reinforces the previous conclusion. Accordingly, still at LPSP = 0, CAPEX equals 22.8 k$ for 5 PV panels, 23.0 k$ at 10 PV panels, and 25.5 k$ at 15 PV panels (Figure 16). Additionally, this also confirms that 10 panels would be enough.
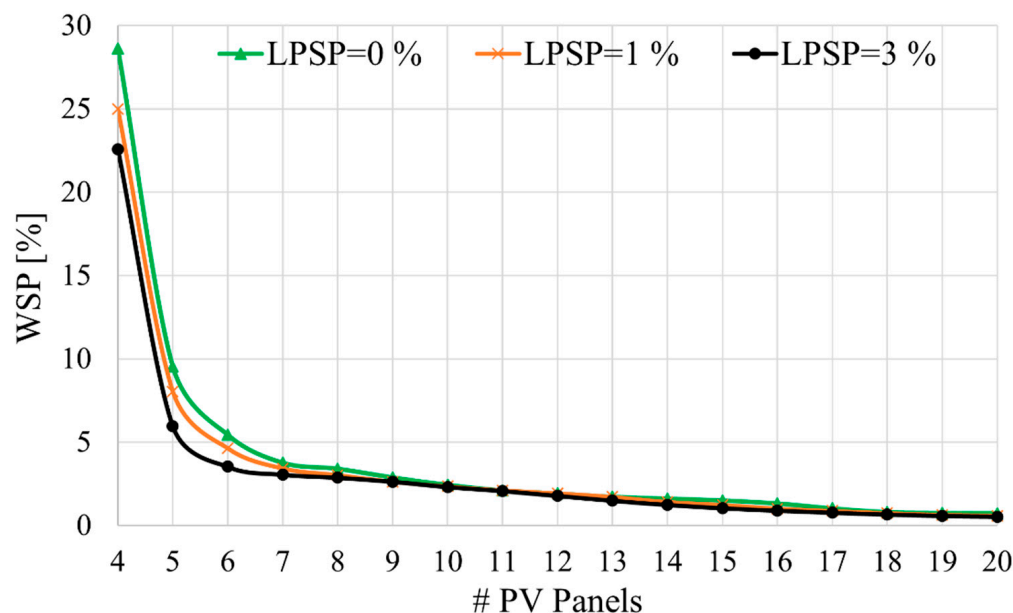

Figure 15. Comparison of different WSP values for three LPSP tolerances of 0, 1%, and 3%.

As another example, at LPSP of 3%, for 5 PV panels, the LCOE is 0.85 $/kWh and reduces to 0.60 $/kWh for 10 PV panels and to 0.56 $/kWh at 15 PV panels (Figure 14). Furthermore, WSP values for these panel numbers are 6.0%, 2.3%, and 1.0%, respectively (Figure 15). Additionally, finally, CAPEX (Figure 16) equals 9.6 k$, 13.6 k$, and 18.9 k$ for 5, 10, and 15 PV panels, respectively. Here, we see that a higher tolerance to a loss of power could lead to substantial savings: the LCOE could be reduced by more than 50% when LPSP increases from 0 to 3%, especially for small systems, and the WSP would

also drop. This could sound counter-intuitive, but when people accept several potential periods without electricity (higher LPSP), this provides energy to fill the water tank and thus reduces the WSP. Finally, the CAPEX also drops with higher LPSP.
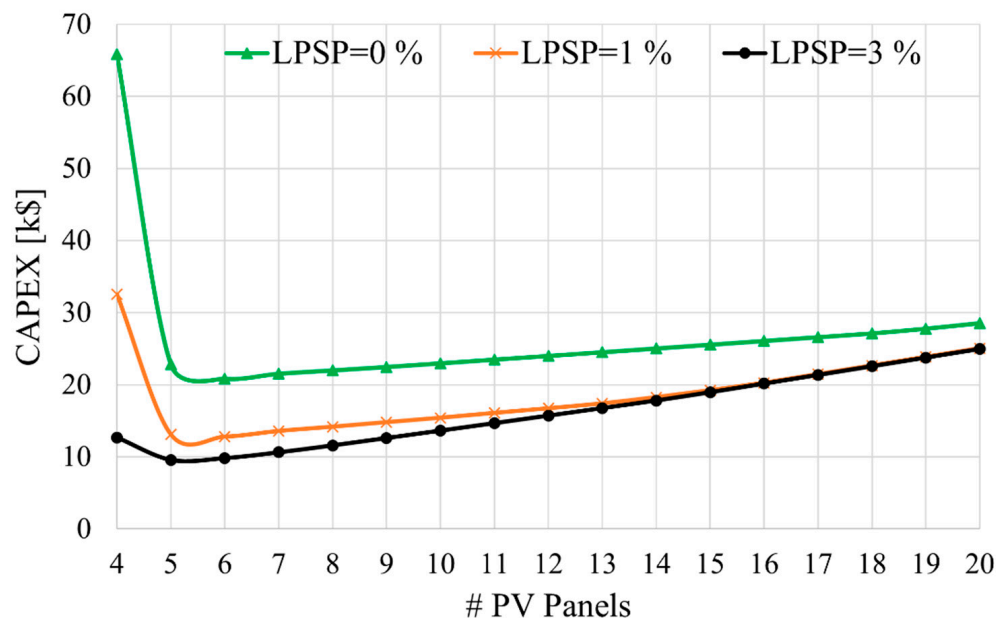

Figure 16. Comparison of different investment costs for three LPSP tolerances of 0, 1%, and 3%.

These graphs (Figures 14–16) provide a clear picture of the effect of LPSP and WSP tolerances on sizing and the cost of system. For instance, if investment cost is a concern of the user of the system, selecting a system with PV panels of 6 to 9 would be reasonable since, in these sizes, CAPEX does not increase considerably, but WSP reduces from 5.5% up to 2.9% at LPSP of 0. Additionally, similarly, from 4.6% up to 2.6% at LPSP of 1%, and from 3.5% up to 2.6% at LPSP of 3%.

4. Conclusions

In this study, photovoltaic electrification and water pumping based on a PV-battery system were investigated for a city located in southern Iran, i.e., Bandar-Abbas. Two specific concepts that influence the size and cost of the system were used herein: (1) the water shortage probability (WSP) for the evaluation of drought tolerance in the context of irrigation; and (2) the loss of power supply probability (LPSP) as a tolerance threshold for lack of access to electricity of a rural home. Moreover, a simplified expression for the levelized cost of energy (LCOE) was also implemented to evaluate the financial viability of systems with more than the sole capital expenditure (CAPEX). A MATLAB genuine implementation of a particular electrification/pumping algorithm was carried out. Then, the correct formulation and implementation were validated against a benchmark solution. Additionally, finally, a case study involving parametric variations was undertaken.

The investigations were carried out to determine the appropriate size of the system (in terms of the number of PV panels and the battery capacity required) for selected values of LPSP and to find the corresponding values of WSP, LCOE, and CAPEX.

The results, not surprisingly, revealed that increasing the number of PV panels leads to more energy production and consequently lower WSP. This, however, is at the expense of more investment in the system (CAPEX). However, the effect of increasing energy production may increase the capital cost but leads to the reduction of the LCOE.

Several preponderantly interesting results were found here:

- A comparison of different LPSPs shows that a small increase in tolerance for power loss can considerably lower the size, cost, and the LCOE of the system with limited change in water shortage probabilities. This suggests that communities and/or dwellings

with limited financial capabilities should consider complementary strategies to avoid running out of water for irrigation.

- The WSP could go lower with higher LPSP because more water could be pumped into the tank when people can tolerate power shortages.
- There is a minimum in the curve that plots the CAPEX with respect to the number of PV panels in the system where limited variations of WSP and LCOE happen with further increases in the number of PV panels and that for any LPSP. This is due to the battery bank requirement rapid increase below the minimal number of panels which are less expensive. For the current study, this is about 5 to 6 panels.

5. Perspectives

The current work undertaken in the t3e group and ÉTS Montreal now is concerned with electrification/pumping and treating/heating water for the domestic needs of a small size remote community. Namely, the investigation aims at defining the appropriate size of a system with respect to community size, needs, budget, and tolerances to water and power shortages.

Another crucial work that remains to be done is to determine the influence of two different business models to satisfy the same needs: (1) the individual or the community owns the system; or (2) a company installs a system and sells electricity and water to consumers. These two diametrically opposed models could lead to very different systems for the same communities because low LPSPs imply that a large amount of water could be pumped unnecessarily due to too limited reservoirs. This remains to be explored.

Finally, if the conventional battery is appropriate for small-scale systems, when the irrigation component becomes more important, it would be interesting to consider other energy storage modes both in terms of their technical and environmental performance.

Nomenclature

Symbols:

A, B, C	Arguments of θ
CAPEX	Capital expenditure [$]
d	Number of the day (from 1 to 365)
EP_t	Electricity production in year t [kWh]
F_t	Fuel cost [$]
G	Incident solar irradiation [W/m^2]

G_{STC}	Incident solar irradiation on STC [W/m^2]
g	Gravitational acceleration [m/s^2]
H	Total dynamic head [m]
I_β	Global solar radiation on an inclined surface [W/m^2]
I_b	Direct beam radiation [W/m^2]
I_d	Diffusive radiation [W/m^2]
I_{0-pv}	Investment cost of PV panel [$/W]
I_{0-pump}	Investment cost of pump [$/W]
I_{PV}	Current of the panel [A]
I	Global horizontal irradiance [W/m^2]
$I_{PV,r}$	Rated current of the panel [A]
M_t	Scheduled maintenance cost [$]
n	Number of the day
N_{PV}	Number of PV panels
N_{PV} *max*	Maximum number of PV panels
$OPEX_t$	Operational expenditure [$]
O_t	Unscheduled operational cost [$]
P_{PV}	Output power of the PV panel [W]
P_l	Load power [W]
r	Real discount rate [%]
R_t	Replacement cost [$]
$R_{inverter}$	Replacement cost of inverter [$]
$R_{battery}$	Replacement cost of battery [$]
T_{amb}	Ambient temperature [°C]
R_b	Geometric factor
T_C	Temperature of panel [°C]
$T_{C,STC}$	Temperature of the cell at STC [°C]
t	Time [hour]
V_{PV}	Voltage of the panels [v]
θ	Angle of incidence [°]
$\dot{V}$	Volumetric flow rate [m^3/s]

Greek characters:

β	Tilt angle [°]
σ	Hourly self-discharge rate
ρ	Density [kg/m^3]
α	Temperature coefficient [%/°C]
π	Pumping power [W]
η_{bc}	Efficiency of battery at charge mode [%]
η_{bd}	Efficiency of battery at discharge mode [%]
η_{inv}	Efficiency of inverter [%]
θ_z	Zenith angle [°]
μ	Albedo coefficient
δ	Declination angle [°]
ω_{ss}	Sunset hour angle [°]
ω_{sr}	Sunrise hour angle [°]
φ	Latitude [°]
ω	Hour angle [°]
Γ	Argument of EOT
λ	Longitude [°]
γ	Azimuth angle [°]

Abbreviations

CWR	Crop Water Requirement [mm]
DNI	Direct Normal irradiation [W/m^2]
EOT	Equation of Time
IWR	Irigation Water Requirement [mm]
IBC	Installed Battery Capacity [kWh]
IODC	Indian Ocean Data Coverage

LCOE	Levelized Cost of Energy [$/kWh]
LL	Local Longitude [°]
LT	Local Time
LSTM	Local Standard Time Meridian
LPSP	Loss of Power Supply Probability [%]
LPS	Loss of Power Supply [W]
NOCT	Nominal Operating Cell Temperature [°C]
NSRDB	National Solar Radiation Database
PSM-v3	Physical Solar Model Version 3
PV	Photovoltaic
STC	Standard Test Condition
ST	Solar Time
WSP	Water Shortage Probability [%]
WS	Water shortage [m^3]

References

1. *Key World Energy Statistics 2021*; International Energy Agency: Paris, France, 2021.
2. Chapin, D.M.; Fuller, C.S.; Pearson, G.L. A New Silicon *p-n* Junction Photocell for Converting Solar Radiation into Electrical Power. *J. Appl. Phys.* **1954**, *25*, 676. [CrossRef]
3. Gualteros, S.; Rousse, D.R. Solar water pumping systems: A tool to assist in sizing and optimization. *Sol. Energy* **2021**, *225*, 382–398. [CrossRef]
4. IRENA. *Rethinking Energy 2017: Accelerating the Global Energy Transformation*; International Renewable Energy Agency: Abu Dhabi, United Arab Emirates, 2017.
5. Bhayo, B.A.; Al-Kayiem, H.H.; Gilani, S.I. Assessment of standalone solar PV-Battery system for electricity generation and utilization of excess power for water pumping. *Sol. Energy* **2019**, *194*, 766–776. [CrossRef]
6. Vishnupriyan, J.; Partheeban, P.; Dhanasekaran, A.; Shiva, M. Analysis of tilt angle variation in solar photovoltaic water pumping system. *Mater. Today Proc.* **2022**, *58*, 416–421. [CrossRef]
7. Tiwari, A.K.; Kalamkar, V.R.; Pande, R.R.; Sharma, S.K.; Sontake, V.C.; Jha, A. Effect of head and PV array configurations on solar water pumping system. *Mater. Today Proc.* **2020**, *46*, 5475–5481. [CrossRef]
8. Raza, F.; Tamoor, M.; Miran, S.; Arif, W.; Kiren, T.; Amjad, W.; Hussain, M.I.; Lee, G.-H. The Socio-Economic Impact of Using Photovoltaic (PV) Energy for High-Efficiency irrigation Systems: A Case Study. *Energies* **2022**, *15*, 1198. [CrossRef]
9. Khan, M.S.; Tahir, A.; Alam, I.; Razzaq, S.; Usman, M.; Tareen, W.U.K.; Baig, N.A.; Atif, S.; Riaz, M. Assessment of Solar Photovoltaic Water Pumping of WASA Tube Wells for irrigation in Quetta Valley Aquifer. *Energies* **2021**, *14*, 6676. [CrossRef]
10. Lunel, T.R.; Rousse, D.R. pvpumpingsystem: A Python package for modeling and sizing photovoltaic water pumping systems. *J. Open Source Softw.* **2020**, *5*, 2637. [CrossRef]
11. Gorjian, S.; NematZadeh, B.; Eltrop, L.; Shamshiri, R.R.; Amanlou, Y. Solar photovoltaic power generation in Iran: Development, policies, and barriers. *Renew. Sustain. Energy Rev.* **2019**, *106*, 110–123. [CrossRef]
12. Renewable Energy and Energy Efficiency Organization (SATBA). Available online: http://www.satba.gov.ir/en/home (accessed on 1 August 2021).
13. Nikzad, A.; Chahartaghi, M.; Ahmadi, M.H. Technical, economic, and environmental modeling of solar water pump for irrigation of rice in Mazandaran province in Iran: A case study. *J. Clean. Prod.* **2019**, *239*, 118007. [CrossRef]
14. Iran's Ministry of Energy-Tavanir Holding Company of Iran. Detailed Statistics of Iran Electricity Production Industry. August 2021. Available online: https://amar.tavanir.org.ir/en/ (accessed on 1 August 2021).
15. Niajalili, M.; Mayeli, P.; Naghashzadegan, M.; Poshtiri, A.H. Techno-economic feasibility of off-grid solar irrigation for a rice paddy in Guilan province in Iran: A case study. *Sol. Energy* **2017**, *150*, 546–557. [CrossRef]
16. Shahverdi, K.; Bellos, E.; Loni, R.; Najafi, G.; Said, Z. Solar-driven water pump with organic Rankine cycle for pressurized irrigation systems: A case study. *Therm. Sci. Eng. Prog.* **2021**, *25*, 100960. [CrossRef]
17. Rizi, A.P.; Ashrafzadeh, A.; Ramezani, A. A financial comparative study of solar and regular irrigation pumps: Case studies in eastern and southern Iran. *Renew. Energy* **2019**, *138*, 1096–1103. [CrossRef]
18. Chahartaghi, M.; Nikzad, A. Exergy, environmental, and performance evaluations of a solar water pump system. *Sustain. Energy Technol. Assess.* **2020**, *43*, 100933. [CrossRef]
19. NSRDB. The National Solar Radiation Database. Available online: https://maps.nrel.gov/nsrdb-viewer/ (accessed on 1 August 2021).
20. Duffie, J.A.; Beckman, W.A. *Solar Engineering of Thermal Processes*; John Wiley & Sons, Inc.: Hoboken, NJ, USA, 2013.
21. Cooper, P. The absorption of radiation in solar stills. *Sol. Energy* **1969**, *12*, 333–346. [CrossRef]
22. Ibrahim, I.A.; Khatib, T.; Mohamed, A. Optimal sizing of a standalone photovoltaic system for remote housing electrification using numerical algorithm and improved system models. *Energy* **2017**, *126*, 392–403. [CrossRef]
23. ABukar, A.L.; Tan, C.W.; Lau, K.Y. Optimal sizing of an autonomous photovoltaic/wind/battery/diesel generator microgrid using grasshopper optimization algorithm. *Sol. Energy* **2019**, *188*, 685–696.

24. *Valve-Regulated Lead-Acid (VRLA): Gelled Electrolyte (gel) and Absorbed Glass Mat (AGM) Batteries*; EAST PENN Expertise and American Workmanship: Lyons, PA, USA, 2007.
25. Li, H.; Sun, Y. Operational performance study on a photovoltaic loop heat pipe/solar assisted heat pump water heating system. *Energy Build.* **2018**, *158*, 861–872. [CrossRef]
26. Numbi, B.; Malinga, S. Optimal energy cost and economic analysis of a residential grid-interactive solar PV system- case of eThekwini municipality in South Africa. *Appl. Energy* **2017**, *186*, 28–45. [CrossRef]
27. Bhandari, R.; Stadler, I. Grid parity analysis of solar photovoltaic systems in Germany using experience curves. *Sol. Energy* **2009**, *83*, 1634–1644. [CrossRef]
28. Ndwali, K.; Njiri, J.G.; Wanjiru, E.M. Multi-objective optimal sizing of grid connected photovoltaic batteryless system minimizing the total life cycle cost and the grid energy. *Renew. Energy* **2019**, *148*, 1256–1265. [CrossRef]
29. Komiyama, R.; Fujii, Y. Long-term scenario analysis of nuclear energy and variable renewables in Japan's power generation mix considering flexible power resources. *Energy Policy* **2015**, *83*, 169–184. [CrossRef]
30. Komiyama, R.; Fujii, Y. Assessment of massive integration of photovoltaic system considering rechargeable battery in Japan with high time-resolution optimal power generation mix model. *Energy Policy* **2014**, *66*, 73–89. [CrossRef]
31. Li, Y.; Gao, W.; Ruan, Y.; Ushifusa, Y. The performance investigation of increasing share of photovoltaic generation in the public grid with pump hydro storage dispatch system, a case study in Japan. *Energy* **2018**, *164*, 811–821. [CrossRef]
32. Besarati, S.M.; Padilla, R.V.; Goswami, D.Y.; Stefanakos, E. The potential of harnessing solar radiation in Iran: Generating solar maps and viability study of PV power plants. *Renew. Energy* **2013**, *53*, 193–199. [CrossRef]
33. Chandler, W.; Whitlock, C.; Stackhouse, P. *A Renewable Energy Resource Web Site (Release 6.0)*; NASA Surface Meteorology and Solar Energy (SSE): Washington, DC, USA, 2015.
34. Pereira, L.; Alves, I. *Crop Water Requirements*; International Commission on Agricultural Engineering (CIGR): Lisbon, Portugal, 2005.
35. Bazrafshan, O.; Zamani, H.; Etedali, H.R.; Dehghanpir, S. Assessment of citrus water footprint components and impact of climatic and non-climatic factors on them. *Sci. Hortic.* **2019**, *250*, 344–351. [CrossRef]
36. Memme, S.; Fossa, M. Maximum energy yield of PV surfaces in France and Italy from climate based equations for optimum tilt at different azimuth angles. *Renew. Energy* **2022**, *200*, 845–866. [CrossRef]